

LVSA: Training-Free Sparse Attention for Long Video Diffusion

Gael Glorian ^{*}¹, Ioannis Lamprou ¹, Zhen Zhang ¹, Yujie Yuan¹, and Hongsheng Liu ²

¹Distributed Parallel Technology Laboratory, Paris Research Center, Huawei Technologies France

²AI Framework and Data Technology Lab, Huawei Technologies Co., Ltd.

Abstract

Dense self-attention is the compute and quality bottleneck of long-video diffusion inference: cost grows quadratically with the sequence length, and beyond the training horizon the model converges to near-static output, that is, “frozen” repetitive video. State of the art approaches are either too costly, e.g., they require retraining, or fail to satisfy both performance and quality objectives in a scalable manner. To this end, we introduce Long Video Sparse Attention (LVSA), a training-free model-agnostic block-sparse attention for video diffusion transformers that combines a structured window pattern with rotating global anchors, thus removing the fixed-grid bias which causes long-range temporal artifacts. LVSA, combined with a FlashInfer kernel, reduces compute up to 3.17× on Wan 2.1 1.3B at a 6× horizon, 2.98× on Wan 2.1 14B at a 6× horizon, and 3.33× on HunyuanVideo 1.5 at a 1.5× horizon, compared to dense attention. Beyond reducing compute, LVSA enables HunyuanVideo 1.5 generation at a 2× horizon, which is otherwise out-of-memory on a single GPU. Moreover, LVSA provides speedups up to 2.41× compared to RIFLEx [13] and 3.27× compared to UltraViCo [14] on Wan 2.1 1.3B. To demonstrate applicability across diverse platforms, we apply LVSA on NPUs and achieve speedups up to 2.71× on Wan 2.2 A14B and 3.24× on Wan 2.1 1.3B compared to dense attention. To evaluate quality in a fair way, we introduce VQeval, a tool properly scoring loopy video failures, which instead are rewarded in state of the art evaluators like VBench-Long [1]. LVSA is quality-neutral for generation at training horizon length and quality-positive at extended lengths. **code:** <https://github.com/JiusiServe/LongVideoSparseAttention>

1 Introduction

Video diffusion transformers (DiTs) like Wan [5] and HunyuanVideo [3] have set new bars for text-to-video generation quality, but inference costs rise steeply with the number of generated frames as standard self-attention brings about quadratic compute. At the 14-billion parameter scale, KV memory is pushed near the 80 GB GPU envelope thus making longer video generation infeasible. Moreover, with respect to video quality, beyond the training horizon of 81 frames for Wan and 129 frames for HunyuanVideo, dense attention produces frozen or looping video, which is of very low quality by an observant’s standards.

The above compute and quality challenges have captured the interest of the research community [6]. Sparse VideoGen [7, 9], AdaSpa [8], Sliding Tile Attention [12], and Radial Attention [4] all target the quadratic cost of video self-attention with training-free block or windowed patterns. Yet, the long-range temporal-repetition failures are still hard to eliminate. On the other hand, approaches on video extrapolation with quality preservation fail to deescalate the compute cost: RIFLEx [13] modifies a single temporal RoPE frequency to extend the training horizon, while UltraViCo [14] applies a per-pair logit decay via a fused Sage Attention [11] kernel. Note, in this paper, we consider a single-scene scenario.

In this work, we seek to address these shortcomings and harness the tradeoff between compute and quality. To do so, we make the following contributions:

- We introduce Long-Video Sparse Attention (**LVSA**), a training-free block-sparse model-agnostic attention algorithm comprising novel rotating sparse patterns and expanded adaptive window logic.
- We introduce a custom evaluation benchmark, namely **VQeval**, to properly score loopy video failures, in contrast to state of the art VBench-Long [1].

^{*}Corresponding author: gael.glorian@huawei.com

- We experimentally validate the efficacy of our approach across three architecturally distinct video DiTs for inference on a single 80GB GPU. LVSA combined with a FlashInfer kernel delivers a $3.17\times$ speedup on Wan 2.1 1.3B, $2.98\times$ on Wan 2.1 14B, and $3.33\times$ on HunyuanVideo 1.5 at the longest tested generation horizon per model, while significantly outscoring dense attention on VQeval at a $6\times$ horizon on both Wan models. LVSA additionally enables HunyuanVideo 1.5 generation at a $2\times$ horizon (257 frames), where dense attention is infeasible due to memory exhaustion. LVSA outperforms UltraViCo and RIFLEx both in compute (up to $3.27\times$) and quality.
- We showcase the efficacy of LVSA for video generation on NPUs. We achieve a $2.71\times$ speedup on Wan 2.2 A14B and $3.24\times$ speedup on Wan 2.1 1.3B at a $6\times$ horizon, with good video quality.
- We include our implementation as a plugin in a popular open-source platform.

2 Method

A video diffusion transformer operates on a latent video tensor patchified into a sequence of $N = T \cdot P$ tokens, each of dimension d , where T is the number of latent temporal frames, from now on simply referred to as *frames*, and $P = H_p \cdot W_p$ is the number of spatial patches (height times width) per frame. Below, let $t \in \{0, 1, \dots, T-1\}$ denote the t -th frame and $q_{t,p}, k_{t,p}, v_{t,p}$ denote the p -th query, key, and value, tokens for frame t , where $p \in \{0, 1, \dots, P-1\}$. The (spatio-temporal) self-attention formula for a query token $q_{t,i}$ is

$$\text{Attn}(q_{t,i}) = \sum_{\tau=0}^{T-1} \sum_{p=0}^{P-1} \frac{\exp(q_{t,i} \cdot k_{\tau,p} / \sqrt{d})}{\sum_{\tau'=0}^{T-1} \sum_{p'=0}^{P-1} \exp(q_{t,i} \cdot k_{\tau',p'} / \sqrt{d})} \cdot v_{\tau,p}. \quad (1)$$

The (dense) attention cost for $\text{Attn}(q_{t,i})$ is $O(Nd) = O(TPd)$. The formula must be computed for each i and t , which leads to a prohibitive $O(N^2d)$ complexity for long video generation. Note that each query frame attends to all other frames in the temporal dimension T . Let us formalize and generalize this notion of per-frame attention.

Definition 1 For a query frame t , the set of frames it attends to is denoted by $\mathcal{A}(t) \subseteq \{0, 1, \dots, T-1\}$. In dense attention, $\mathcal{A}(t) = \{0, 1, \dots, T-1\}$, that is, t attends to all frames.

To enable long video generation of high quality quickly, we introduce sparsity logic. We seek to restrict the set of frames a query frame attends to. Thus, we perform fewer computations, yet in a smart way to avoid sacrificing quality. We generalize the above self-attention formula to:

$$\text{Attn}(q_{t,i}) = \sum_{\tau \in \mathcal{A}(t)} \sum_{p=0}^{P-1} \frac{\exp(q_{t,i} \cdot k_{\tau,p} / \sqrt{d})}{\sum_{\tau' \in \mathcal{A}(t)} \sum_{p'=0}^{P-1} \exp(q_{t,i} \cdot k_{\tau',p'} / \sqrt{d})} \cdot v_{\tau,p}. \quad (2)$$

Note the complexity to compute $\text{Attn}(q_{t,i})$ is $O(|\mathcal{A}(t)|Pd)$. The question that now remains is to define $\mathcal{A}(t)$ for each frame t .

Let us now define our attention pattern for each query frame t , which comprises two components. To maintain quality throughout time, we let each query frame attend to a set of (global) frames at key times during the whole time horizon. Also, each frame attends to a small (local) window of frames surrounding it temporally. Overall, we wish for each frame to attend to a sensible yet small number of frames, both locally and globally, such that compute is reduced, while quality is not compromised.

Definition 2 The Long Video Sparse Attention (LVSA) formula is the spatio-temporal attention formula defined in Equation 2 with $\mathcal{A}(t) = G \cup \mathcal{W}(t)$, where

- $G = \{t \mid t = 0, 1, \dots, T-1 \wedge t \bmod T_{\text{per}} = 0\}$ are equidistant global frames at a period $T_{\text{per}} \in \mathbb{N}$,
- $\mathcal{W}(t) = \{t' \mid w_{lo}(t) \leq t' \leq w_{hi}(t)\}$ is a local window of frames around t with $w_{lo}(t) = \max\{0, t-W\}$ and $w_{hi}(t) = \min\{T-1, t+W\}$, where $W \in \mathbb{N}$ is the window size and we assume $2W+1 \leq T$.

For a visual depiction of Definition 2, see Figure 1a. Note frame 0 is always a global anchor, thus ensuring queries always attend to scene-establishing content.

Following the above definition, the user must specify T_{per} and W to compute the formula on the globally and locally attended frames. The question arises on how to select these parameters. For

simplicity of exposition we present LVSA with a single global set G of equidistant frames; an extension including more dedicated initial anchors is a straightforward generalization.

To avoid fluctuations in compute, and maintain a constant budget per query frame, we fix a target budget C and let $|\mathcal{A}(t)| \approx C$, for each frame t , with deviation bounded by integer keyframe-spacing rounding (at most ± 2 frames across the configurations we evaluate). By default, we let C be equal to the reference frame count of the trained model, e.g., $C = \frac{81-1}{4} + 1 = 21$ frames for Wan 2.1 1.3B, as Wan is trained on an 81-frame horizon and has its variational auto encoder (VAE) factor set to 4. Intuitively, since the model is trained on a budget of C frames, we use the same budget for inference. Using a smaller budget would improve efficiency, yet lower quality, while using a larger budget would be costly and eventually intractable. Overall, the complexity of $\text{Attn}(q_{t,i})$ becomes $O(CPd)$, for each frame t and patch i , yielding a total complexity of $O(TCP^2d)$. The latter is asymptotically *linear* in the number of frames T , thus enabling long video generation.

One could allocate the attention budget C in any way, as long as $|\mathcal{A}(t)| \approx C$ for all t . In our case, we assume W is already fine-tuned, see Section 3. We allocate the remaining budget to the periodic global frames in G and respectively set $T_{\text{per}} = \left\lceil \frac{T}{C-(2W+1)} \right\rceil$. This assignment applies to the practical case where $C > 2W + 1$. Since T_{per} is an integer, the realized $|G| = \lceil T/T_{\text{per}} \rceil$ may differ from the target $C - (2W + 1)$ by up to $T_{\text{per}} - 1$ frames; in our experiments this is at most two frames in either direction.

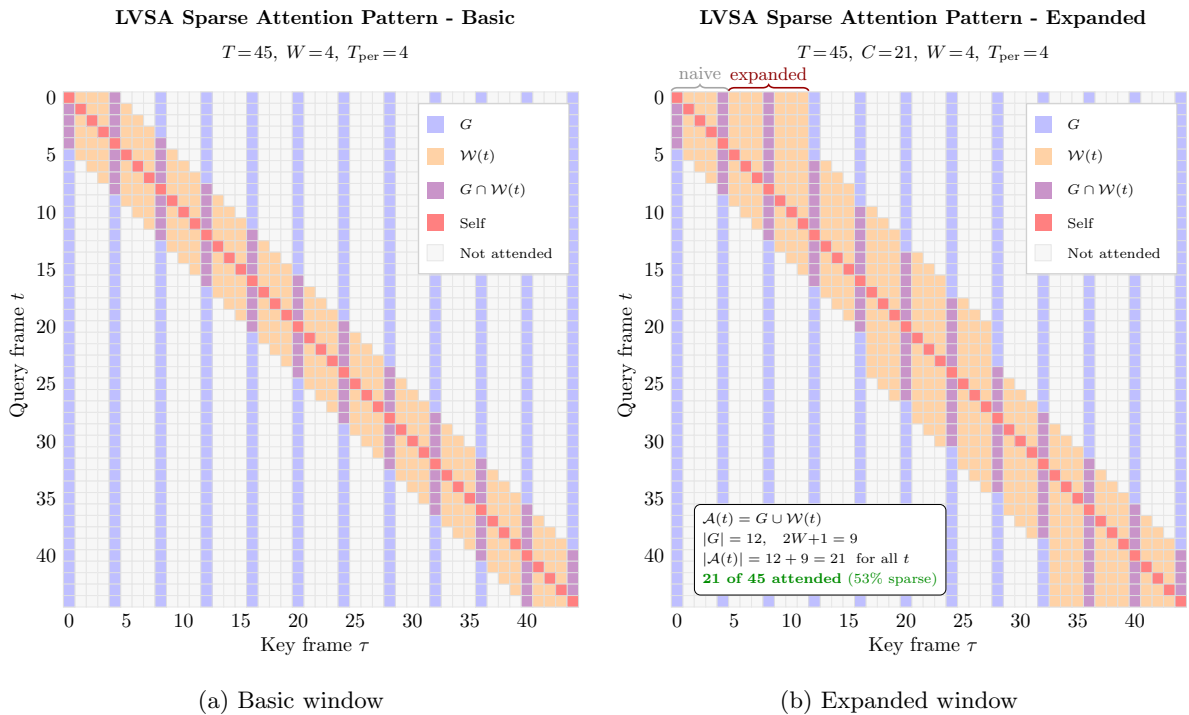


Figure 1: Basic versus expanded window pattern. The basic adaptive window (a) wastes attention budget when the local window overlaps global frames, leaving the per-query attended set below the target C . Expanded bounds (b) account for this overlap by extending the window when needed, so every query frame attends to $|\mathcal{A}(f)| = |G| + \min(2W + 1, T - |G|) \approx C$ unique frames.

Overlapping frames. We now consider the case where $G \cap W(t) \neq \emptyset$ and so some frames are included in both sets. A naive local window, as given in Definition 2, clips at sequence boundaries, giving edge frames a smaller attention budget than interior ones. A simple adaptive window shifts the range appropriately in order to maintain a constant window size for edge cases by setting $w'_{\text{lo}}(t) = \max(0, \min(t - W, T - 1 - 2W))$ and $w'_{\text{hi}}(t) = \min(T - 1, \max(t + W, 2W))$. Thus, every frame attends to exactly $2W + 1$ window frames.

However, when window frames overlap global frames, the effective number of unique non-global frames in the window is reduced, wasting attention budget. We introduce *expanded window bounds* to compensate for this overlap, see Algorithm 1 and Figure 1b.

The cost of Algorithm 1 is negligible, since in practice only a few iterations of the while loop will take place. The algorithm runs on CPU during metadata building and does not enter the attention critical

Algorithm 1 Expanded window bounds for $\mathcal{W}(t)$

Require: Frame t , global frames G , window size W , total frames T **Ensure:** Assign expanded windows bounds (w_{lo}, w_{hi})

- 1: $(l, h) \leftarrow (w'_{lo}(t), w'_{hi}(t))$
 - 2: $target \leftarrow \min(2W+1, T - |G|)$
 - 3: $nonglobal \leftarrow |\{t' \in [l, h] \mid t' \notin G\}|$
 - 4: **while** $nonglobal < target \wedge (l > 0 \vee h < T-1)$ **do**
 - 5: extend the side with the most room by 1; increment $nonglobal$ if the new frame is $\notin G$
 - 6: **end while**
 - 7: $(w_{lo}, w_{hi}) \leftarrow (l, h)$
-

path. With expanded bounds, the total unique attended frames satisfy $|\mathcal{A}(t)| = |G| + \min(2W+1, T - |G|)$ for each frame t , giving a uniform per-frame attention budget across the sequence. For any $T \geq 2W+1$, every query frame t has $|\mathcal{A}(t)| \in [C - \delta, C + \delta]$ with $\delta \leq T_{\text{per}} - 1$, and $|\mathcal{A}(t)|$ is constant across t for fixed G . Empirically, across all configurations used in our experiments, the loop runs at most 8 iterations per call (mean 1.21) and the full per-frame call takes $\approx 1.4 \mu\text{s}$ on a single CPU core. A complete metadata rebuild for a denoising step takes less than $200 \mu\text{s}$, which is negligible compared to the GPU attention kernel.

Rotating periodic global frames. Fixing the periodic global frames in G allows for maintaining information throughout the video duration. Nonetheless, it also creates a persistent bias: these frames are always attended to globally, while intermediate frames are only observed through local windows. Over the course of S denoising steps, the model’s representation of frames not in G is systematically impoverished. At extended lengths, this manifests as long-range temporal artifacts, e.g., repetition, identity drift, etc.

To address this, we introduce *rotating periodic global frames*. At denoising step $s = 0, 1, \dots, S-1$, the global set G^s is different than at previous steps. We shift the members of G by s modulo T_{per} positions and define the set as a function of the denoising step as

$$G^s = \{(s \bmod T_{\text{per}} + i \cdot T_{\text{per}}) \bmod T \mid i = 0, 1, \dots, \lceil T/T_{\text{per}} \rceil - 1\}. \quad (3)$$

See Figure 2 for a visual depiction.

Two properties make this rotation principled. First, over any T_{per} consecutive denoising steps, every frame appears in G^s for at least one value of s , so every frame serves as a global anchor at least once per cycle, eliminating the fixed-grid bias (when T is not a multiple of T_{per} , the last wrap may revisit at most $T_{\text{per}} - 1$ frames within a cycle; this is empirically negligible at the keyframe-spacings used in our experiments). Second, the modular wrapping ensures $|G^s| = \lceil T/T_{\text{per}} \rceil$ is constant across s , so the per-step attention budget does not change.

At each step we recompute the derived index structures for the rotated pattern. This is pure CPU index arithmetic over T elements (T ranges from 21 at a $1\times$ Wan horizon to 121 at a $6\times$ horizon) and takes less than 1 ms per step, which is negligible compared to the GPU attention kernel.

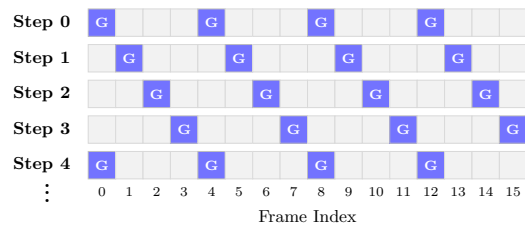


Figure 2: Rotating periodic global frames with $T_{\text{per}} = 4$. The set G^s shifts by one position per denoising step and wraps modulo T . Over any T_{per} consecutive steps, each frame appears as a global anchor exactly once.

3 Experiments on GPU

Models. We experiment with three architecturally distinct video DiTs: (i) **Wan 2.1 T2V-1.3B** – single-stream, 1D RoPE, T5 encoder, 40 steps, (ii) **Wan 2.1 T2V-14B** – same architecture at 14B parameters, 40 steps, and (iii) **HunyuanVideo 1.5 (480p)** – dual-stream, 3D RoPE, Qwen2.5-VL encoder, 50 steps.



Figure 3: HunyuanVideo 1.5 at $2\times$ horizon (257 frames), generated by LVSA-FI on a single 80GB GPU; dense attention is infeasible at this setting due to OOM (Table 1). Frames 32, 96, 160, 224 from the prompt `coral_reef` (best-VQeval prompt at this cell, composite 62.9).

Hardware. A single GPU with 80 GB, PyTorch 2.8/CUDA 12.8.

Video lengths. 480×832 resolution. Wan: 81 ($1\times$ horizon), 161 ($2\times$), 241 ($3\times$), 321 ($4\times$), 401 ($5\times$), 481 ($6\times$) video frames. HunyuanVideo: 65 ($0.5\times$), 129 ($1\times$), 193 ($1.5\times$) and 257 ($2\times$) video frames.

Prompts, seed, and scheduler. We test five diverse long descriptive prompts (around 500 tokens) with seed 16, classifier-free-guidance scale 5.0, and each model’s default scheduler. All cells in Sections 3.1 and 3.2 report mean \pm standard deviation over the 5-prompt set.

Quality Metrics. We report quality results on both **VBench-Long** [1] (subject consistency, temporal flickering, motion smoothness, background consistency, imaging quality) and **VQeval** (dynamic quality, loop quality, text alignment), a custom benchmark we introduce. The two benchmarks are complementary: VBench rewards inter-frame similarity, which scores static or collapsed videos highly, while VQeval’s dynamic and loop dimensions explicitly penalize these failure modes.

3.1 Computational Efficiency

Cross-model scaling. We measure wall time across three models (Wan 2.1 1.3B, Wan 2.1 14B, HunyuanVideo 1.5) and three backends (dense attention, LVSA via scaled-dot-product attention (SDPA), LVSA via FlashInfer block-sparse kernel) over five long descriptive prompts per cell at generation horizons, which are multiples of each model’s training horizon ($2\times$ – $6\times$), see Table 1. At the longest tested horizon per model, LVSA with FlashInfer (LVSA-FI) achieves a **3.17** \times speedup on Wan 2.1 1.3B at a $6\times$ horizon (481 frames; 51 min \rightarrow 16 min), **2.98** \times on Wan 2.1 14B at $6\times$ (238 min \rightarrow 80 min), and **3.33** \times on HunyuanVideo 1.5 at $1.5\times$ (80 min \rightarrow 24 min). The speedup is monotone in horizon and architecture-independent: the same three-model pattern emerges in single-stream/1D-RoPE (Wan) and dual-stream/3D-RoPE (HunyuanVideo) DiTs alike, driven by the quadratic-in- T cost of dense self-attention. At native horizon ($1\times$), LVSA backends are at parity with dense (within $\pm 5\%$ wall time), reflecting the proportionally larger text-encoder cost when video self-attention is short.

Feasibility at the GPU memory ceiling. Beyond speedup, LVSA enables generation that is *infeasible* with dense attention at a fixed GPU memory budget. On HunyuanVideo 1.5 at a $2\times$ horizon (257 frames), dense self-attention runs out of memory on a single 80GB GPU: the SDPA kernel attempts to allocate an additional 19.9 GB on top of a 74.0 GB resident process. LVSA at the same setting caps peak GPU memory at 60.3 GB (SDPA) / 60.4 GB (FlashInfer), leaving ~ 19 GB of headroom and producing decoded video with VQeval composite 60.0 / 58.5 respectively — numbers that have no dense counterpart at this hardware scale. Dense peak memory on HunyuanVideo 1.5 grows from 38.8 GB at a $0.5\times$ horizon to 67.4 GB at $1.5\times$ before exceeding the 80 GB budget at $2\times$. The asymmetric feasibility story — HunyuanVideo 1.5 OOMs at $2\times$ extension while Wan 2.1 14B fits comfortably at $6\times$ (peak 57.8 GB on 481 frames) — is architectural, not parameter-count: both models are ~ 14 B. HunyuanVideo 1.5 is dual-stream, with text-encoder tokens (Qwen2.5-VL + ByT5) participating in self-attention alongside video tokens, whereas Wan’s text enters only via cross-attention. This extends HV’s effective self-attention sequence by the encoder’s output context per layer and pushes its attention activation matrix past the 80 GB budget at $2\times$, while Wan 2.1 14B’s longer (481-frame) but text-free self-attention stays under. Figure 3 shows representative frames from the HV 1.5 $2\times$ LVSA-FI output.

Table 1: Wall time in minutes per video generation on an 80GB GPU, mean over 5 long descriptive prompts. “LVSA-FI” = LVSA with FlashInfer kernel; speedup is LVSA-FI vs. dense attention. HunyuanVideo (HV) 1.5 at a 2× horizon is infeasible for dense attention, while LVSA fits in ≈ 60 GB.

Model	Horizon	Frames	Dense (min)	LVSA (min)	LVSA-FI (min)	Speedup (LVSA-FI)
HV 1.5	0.5×	65	11.6	5.9	5.9	1.97×
HV 1.5	1×	129	37.5	16.7	16.4	2.29×
HV 1.5	1.5×	193	79.7	26.4	23.9	3.33×
HV 1.5	2×	257	OOM	57.9	54.9	∞
Wan 2.1 1.3B	1×	81	2.5	3.1	2.6	0.96×
Wan 2.1 1.3B	2×	161	7.3	6.5	5.1	1.42×
Wan 2.1 1.3B	4×	321	24.0	13.1	10.3	2.32×
Wan 2.1 1.3B	6×	481	50.8	19.9	16.0	3.17×
Wan 2.1 14B	1×	81	12.6	13.5	13.2	0.96×
Wan 2.1 14B	2×	161	35.8	28.5	26.0	1.38×
Wan 2.1 14B	4×	321	114.0	57.8	52.6	2.17×
Wan 2.1 14B	6×	481	237.9	87.2	79.8	2.98×

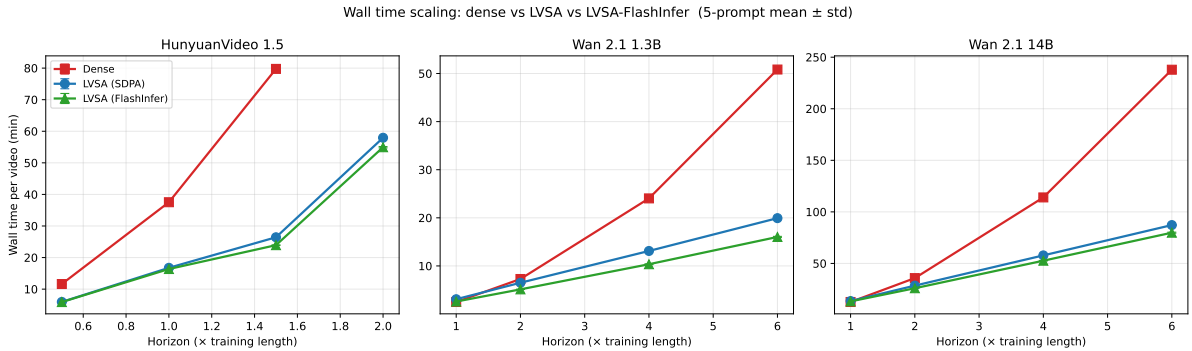


Figure 4: Wall-time scaling across three video DiTs (Wan 2.1 1.3B, Wan 2.1 14B, HunyuanVideo 1.5) for dense attention, LVSA, and LVSA-FI. Speedup grows monotonically with the horizon for all three models; HunyuanVideo 1.5 at 2× horizon (257 frames) has no dense point due to OOM on 80GB GPU.

3.2 Video Quality

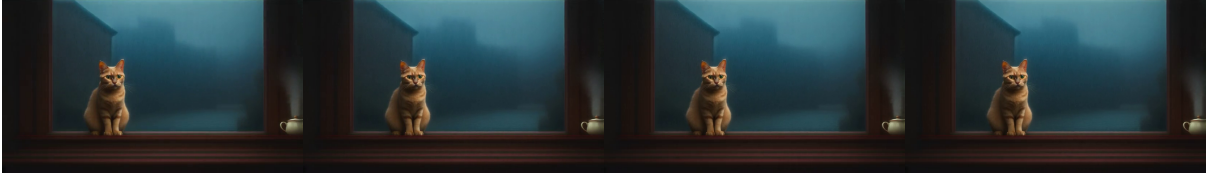
Quality at training horizon. At each model’s reference length (1×), LVSA is quality-neutral with dense attention across all three architectures, see Table 2. VQeval composite is within ± 1.0 of dense on all three models, and VBench-Long composite differences do not exceed 0.014. Both LVSA backends (SDPA and FlashInfer) give equivalent quality at the training horizon, confirming that the attention pattern, and not the kernel choice, determines output quality.

Quality advantage at extended horizons. Beyond the training horizon, LVSA’s VQeval composite consistently outscores dense attention, with the gap widening monotonically with the horizon. On Wan 2.1 1.3B, the LVSA-FI advantage over dense grows from +4.7 at 2× to +11.6 at 4× and +12.1 at 6×. The same pattern holds on Wan 2.1 14B: +3.8 at 2×, +9.7 at 4×, +12.2 at 6×. Across the three architectures, dense attention’s extrapolation failure beyond the training horizon means that dense converges to near-static output with reduced motion variation, which VQeval’s dynamic and loop dimensions properly penalize. LVSA’s sliding-window restriction acts as an implicit regularizer that preserves motion at extended horizons. The VBench-Long composite in Table 2 tells the opposite story: dense scores rise at extended time horizons on both Wan models. The latter is a result of the static-rewarding bias of VBench’s consistency dimensions discussed below.

VBench-Long behavior. VBench-Long’s composite increases for dense attention at extended horizons (Wan 2.1 1.3B 6× dense at 0.891 vs 4× at 0.885 vs 2× at 0.875), because two of its dimensions (`subject_consistency`, `background_consistency`) reward static video and dense attention’s quality collapse at extended horizons produces increasingly frozen output, which VBench credits as “consistent.” At Wan 2.1 1.3B 6× horizon, dense `subject_consistency` reaches 0.991, corresponding to video that is essentially static, while LVSA stays at 0.917, reflecting genuine motion. The motion-independent

Table 2: Quality metrics, mean over 5 long descriptive prompts. VQeval composite is on the $[0, 100]$ scale; VBench-Long composite is on $[0, 1]$. Bold marks the LVSA-FI cells where LVSA-FI matches or exceeds dense at $4\times+$ extension. HunyuanVideo 1.5 at $2\times$ has no dense baseline (OOM, Table 1). The two metrics diverge at Wan extension: dense’s VBench composite *rises* (rewarding its increasingly frozen output) while VQeval correctly tracks the lost motion.

Model	Horizon	Frames	VQeval composite			VBench-Long composite		
			Dense	LVSA	LVSA-FI	Dense	LVSA	LVSA-FI
HV 1.5	$0.5\times$	65	56.9	59.1	57.2	0.887	0.884	0.883
HV 1.5	$1\times$	129	60.5	61.2	60.2	0.893	0.882	0.879
HV 1.5	$1.5\times$	193	61.0	60.9	62.5	0.901	0.897	0.896
HV 1.5	$2\times$	257	OOM	60.0	58.5	OOM	0.898	0.896
Wan 2.1 1.3B	$1\times$	81	56.5	56.5	56.7	0.888	0.888	0.888
Wan 2.1 1.3B	$2\times$	161	55.3	60.1	60.0	0.875	0.869	0.869
Wan 2.1 1.3B	$4\times$	321	50.9	62.1	62.5	0.885	0.869	0.869
Wan 2.1 1.3B	$6\times$	481	48.2	60.1	60.2	0.891	0.852	0.852
Wan 2.1 14B	$1\times$	81	57.2	57.2	58.2	0.909	0.908	0.909
Wan 2.1 14B	$2\times$	161	58.7	62.5	62.5	0.904	0.899	0.900
Wan 2.1 14B	$4\times$	321	55.0	64.7	64.8	0.899	0.893	0.892
Wan 2.1 14B	$6\times$	481	52.7	64.6	64.9	0.886	0.890	0.890



(a) Dense attention (VQeval 37.6, `subject_consistency` 0.991).



(b) LVSA (VQeval 53.1, `subject_consistency` 0.917).

Figure 5: Wan 2.1 1.3B at a $6\times$ horizon (481 frames), prompt `cat_window`, same seed. Frames 20, 200, 380, 460 shown for each backend. Dense converges to near-static output — the cat barely moves across ~ 440 frames — while LVSA produces genuine pose and lighting variation. This is the failure mode VBench-Long’s `subject_consistency` rewards and VQeval correctly penalizes.

`imaging_quality` dimension tells the opposite story: at Wan 2.1 14B $6\times$, LVSA scores 0.598 vs dense 0.522 (+0.076). The VQeval results above therefore correctly capture quality at the horizons where the speedup matters most. Figure 5 makes the frozen-video failure mode visually concrete: dense’s high `subject_consistency` reflects an essentially static output, while LVSA generates real motion at the same horizon, same seed, same prompt.

3.3 Comparison to State of the Art

We compare LVSA head-to-head against two recent training-free extrapolation methods on Wan 1.3B: **RIFLEx** [13], which modifies a single temporal RoPE frequency, and **UltraViCo** [14], which applies a per-pair attention-logit decay with a fused SageAttention kernel. We run UltraViCo via its native `ultra-wan` branch and port RIFLEx to Wan in-house (the reference implementation ships only for HunyuanVideo and CogVideoX). All configurations tested comprise a single 80GB GPU, 50 denoising steps, seed 16, 480×832 , and the same 5-prompt suite. The results are summarized in Table 3. To match UltraViCo’s reference configuration, this comparison uses 50 denoising steps and $84r - 3$ frame counts (165/249/333) where r is the *extrapolation ratio* (training horizon multiplier), versus 40 steps and $80r + 1$ counts (161/321/481) in Table 1. Absolute wall times here are therefore $\sim 25\text{--}30\%$ higher than the corresponding cells in the cross-model sweep (802s vs 618s for LVSA-FI at $4\times$), while LVSA-FI-vs-dense

Table 3: LVSA vs. training-free extrapolation baselines on Wan 2.1 1.3B across 5 long descriptive prompts. VQeval is composite score (mean \pm std); latency is mean seconds per video on a single 80GB GPU. Frame counts (165/249/333) follow UltraViCo’s reference parameterization $84r - 3$. Bold marks the best cell per column.

Method	2 \times (165f)		3 \times (249f)		4 \times (333f)	
	VQeval	latency (s)	VQeval	latency (s)	VQeval	latency (s)
Dense	57.2 \pm 6.4	566	51.1 \pm 4.2	1,145	52.4 \pm 3.5	1,930
RIFLEx	57.8 \pm 7.8	564	51.1 \pm 4.4	1,149	53.6 \pm 3.0	1,931
UltraViCo	62.1 \pm 6.1	741	60.4 \pm 3.8	1,544	58.8 \pm 5.4	2,621
LVSA (SDPA)	64.1 \pm 4.5	502	62.5 \pm 3.8	796	62.4 \pm 1.9	1,021
LVSA-FI	63.7 \pm 5.4	395	62.3 \pm 3.8	621	62.3 \pm 2.2	802
LVSA-FI speedup vs. Dense	1.43 \times		1.84 \times		2.40\times	
LVSA-FI speedup vs. RIFLEx	1.43 \times		1.85 \times		2.41\times	
LVSA-FI speedup vs. UltraViCo	1.88 \times		2.48 \times		3.27\times	

speedup ratios agree within 3% (2.40 \times vs 2.33 \times at 4 \times).

Quality. LVSA achieves the highest VQeval composite at every horizon: +6.5, +11.2, +9.9 over dense at $r = 2/3/4$; +5.9, +11.2, +8.7 over RIFLEx; and +1.7, +1.9, +3.5 over UltraViCo. The gap to dense widens with horizon, consistent with the dense-attention quality collapse documented in Section 3.2: by 4 \times , dense has collapsed (composite 52.4) while LVSA-FI maintains 62.3. RIFLEx alone is statistically indistinguishable from dense on VQeval ($\Delta \in [+0.5, +1.2]$ across ratios, within prompt-level $\sigma \geq 3$) — modifying a single RoPE frequency addresses positional extrapolation but does not prevent the dense-attention quality collapse. UltraViCo’s per-pair logit decay does mitigate the collapse (+4.8 to +9.3 VQeval over dense) but at a steep latency cost (next paragraph), and LVSA still leads it on quality at every ratio. On VBench-Long, dense and RIFLEx edge LVSA on the composite at 4 \times by ~ 0.01 points (driven by `subject_consistency` climbing from 0.949 at 2 \times to 0.986 at 4 \times as dense’s output becomes increasingly frozen — see Section 3.2), but LVSA leads on `imaging_quality` by +0.09 to +0.10 points at every ratio, the only VBench sub-dimension that measures per-frame content independent of temporal stasis. The SDPA and FlashInfer backends of LVSA are quality-equivalent ($|\Delta|_{\text{VQeval}} \leq 0.4$ at every ratio).

Efficiency. LVSA is the only method in this comparison which reduces compute over dense attention. RIFLEx modifies RoPE frequencies only and touches zero attention FLOPs, so its latency is statistically indistinguishable from dense (0.99–1.00 \times , within ± 1 s at every ratio). UltraViCo’s per-pair attention-logit decay requires dense attention over the full $N \times N$ logit matrix and adds kernel overhead: 1.31–1.36 \times dense latency at $r = 2/3/4$. LVSA-FI yields 1.43 \times , 1.84 \times , **2.40 \times** speedup over dense and 1.88 \times , 2.48 \times , **3.27 \times** over UltraViCo at $r = 2/3/4$, at identical VRAM. The FlashInfer kernel contributes a further 1.27–1.28 \times over the SDPA backend at $r \geq 3$ (796s \rightarrow 621s at 3 \times , 1,021s \rightarrow 802s at 4 \times), confirming that block-sparse kernel outperforms the per-frame SDPA Python loop at long sequences.

Orthogonality and composition. RIFLEx modifies RoPE frequencies (different tensor), UltraViCo modifies attention-logit magnitudes, and LVSA modifies attention support. LVSA and RIFLEx operate on fully orthogonal tensors, compose without interaction and produce valid videos with no implementation conflict. Empirically, the composition trades a small amount of VQeval dynamic quality for slightly tighter VBench-Long consistency: LVSA+RIFLEx VQeval is 66.8/65.1/66.8 vs LVSA 67.9/68.1/66.8 at $r = 2/3/4$, while VBench composite moves 0.899/0.884/0.893 vs LVSA 0.873/0.883/0.881. Neither side clearly wins the composition; LVSA’s sparse pattern already captures most of what RIFLEx’s single-frequency rescaling would provide. LVSA and UltraViCo act on the same tensor but on disjoint aspects (support vs. magnitude); a fused implementation applies UltraViCo’s λ_{ij} factor inside LVSA’s sparse kernel.

Table 4: LVSA performance on NPU: Timings refer to iteration time averages in seconds over 40 steps.

(a) Wan 2.1 1.3B				(b) Wan 2.2 A14B			
Frames	Dense	LVSA	Speedup	Frames	Dense	LVSA	Speedup
480 × 832				480 × 832			
161 (2×)	15.71	16.89	0.93×	161 (2×)	10.30	13.16	0.78×
321 (4×)	50.18	32.29	1.55×	321 (4×)	30.89	24.27	1.27×
481 (6×)	103.87	47.76	2.17×	481 (6×)	62.76	35.46	1.77×
720 × 1280				720 × 1280			
161 (2×)	66.45	53.73	1.24×	161 (2×)	40.44	39.22	1.03×
321 (4×)	232.88	103.81	2.24×	321 (4×)	138.87	74.09	1.87×
481 (6×)	499.47	154.27	3.24×	481 (6×)	294.93	108.90	2.71×

4 Experiments on NPU

We port LVSA into vLLM-Omni [10] and provide some initial experimental results, which demonstrate the applicability of LVSA across diverse hardware. For a 40-step inference at a 6× horizon (481 frames) with LVSA (with a standard NPU kernel), we obtain a 2.17× speedup (480 × 832), 3.24× speedup (720 × 1280), and quality-positive result for Wan 2.1-1.3B on one NPU. For Wan 2.2-A14B, 40-step inference on 8 NPUs with an Ulysses [2] sequence parallelism configuration, we obtain a 1.77× speedup (480 × 832), 2.71× speedup (720 × 1280) and quality-positive result. All preliminary results are given in Table 4. Timings are given as iteration time averages in seconds to avoid any pre- and post-processing bias in vLLM-Omni. Timings, and speedups, remain stable across five different complex prompts of possibly different length. In terms of quality, the gap between dense attention and LVSA grows comparatively to the demonstrated one for GPUs in the previous section.

5 Conclusion

We presented LVSA, a training-free block-sparse attention for long-video diffusion inference. We showed the significant benefits of LVSA across diverse models, architectures, and hardware, both on generation performance and quality, and the impact brought about compared to state of the art baselines. Future work may target further performance improvements, as well as generalizing the above benefits to a multi-scene video generation scenario.

References

- [1] Ziqi Huang, Yanan He, Jiashuo Yu, Fan Zhang, Chenyang Si, Yuming Jiang, Yuanhan Zhang, Tianxing Wu, Qingyang Jin, Nattapol Chanpaisit, Yaohui Wang, Xinyuan Chen, Limin Wang, Dahua Lin, Yu Qiao, and Ziwei Liu. VBench: Comprehensive benchmark suite for video generative models. In *Proceedings of the IEEE/CVF Conference on Computer Vision and Pattern Recognition*, 2024.
- [2] Sam Ade Jacobs, Masahiro Tanaka, Chengming Zhang, Minjia Zhang, Shuaiwen Leon Song, Samyam Rajbhandari, and Yuxiong He. Deepspeed ulysses: System optimizations for enabling training of extreme long sequence transformer models. *arXiv preprint arXiv:2309.14509*, 2023.
- [3] Weijie Kong, Qi Tian, Zijian Zhang, Rox Min, Zuozhuo Dai, Jin Zhou, Jiangfeng Xiong, Xin Li, Bo Wu, Jianwei Zhang, et al. Hunyuanvideo: A systematic framework for large video generative models. *arXiv preprint arXiv:2412.03603*, 2024.
- [4] Xingyang Li*, Muyang Li*, Tianle Cai, Haocheng Xi, Shuo Yang, Yujun Lin, Lvmin Zhang, Songlin Yang, Jinbo Hu, Kelly Peng, Maneesh Agrawala, Ion Stoica, Kurt Keutzer, and Song Han. Radial attention: $\mathcal{O}(n \log n)$ sparse attention with energy decay for long video generation. *arXiv preprint arXiv:2506.19852*, 2025.
- [5] Team Wan, Ang Wang, Baole Ai, Bin Wen, Chaojie Mao, Chen-Wei Xie, Di Chen, Feiwu Yu, Haiming Zhao, Jianxiao Yang, Jianyuan Zeng, Jiayu Wang, Jingfeng Zhang, Jingren Zhou, Jinkai Wang, Jixuan Chen, Kai Zhu, Kang Zhao, Keyu Yan, Lianghai Huang, Mengyang Feng, Ningyi Zhang, Pandeng Li, Pingyu Wu, Ruihang Chu, Ruili Feng, Shiwei Zhang, Siyang Sun, Tao Fang, Tianxing Wang, Tianyi Gui, Tingyu Weng, Tong Shen, Wei Lin, Wei Wang, Wei Wang, Wenmeng Zhou, Wenten Wang, Wenting Shen, Wenyan Yu, Xianzhong Shi, Xiaoming Huang, Xin Xu, Yan Kou, Yangyu Lv, Yifei Li, Yijing Liu, Yiming Wang, Yingya

- Zhang, Yitong Huang, Yong Li, You Wu, Yu Liu, Yulin Pan, Yun Zheng, Yuntao Hong, Yupeng Shi, Yutong Feng, Zeyinzi Jiang, Zhen Han, Zhi-Fan Wu, and Ziyu Liu. Wan: Open and advanced large-scale video generative models. *arXiv preprint arXiv:2503.20314*, 2025.
- [6] Faraz Waseem and Muhammad Shahzad. Video is worth a thousand images: Exploring the latest trends in long video generation. *ACM Comput. Surv.*, 58(6), December 2025.
- [7] Haocheng Xi, Shuo Yang, Yilong Zhao, Chenfeng Xu, Muyang Li, Xiuyu Li, Yujun Lin, Han Cai, Jintao Zhang, Dacheng Li, et al. Sparse videogen: Accelerating video diffusion transformers with spatial-temporal sparsity. *arXiv preprint arXiv:2502.01776*, 2025.
- [8] Yifei Xia, Suhan Ling, Fangcheng Fu, Yujie Wang, Huixia Li, Xuefeng Xiao, and Bin Cui. Training-free and adaptive sparse attention for efficient long video generation. In *ICCV*, 2025.
- [9] Shuo Yang, Haocheng Xi, Yilong Zhao, Muyang Li, Jintao Zhang, Han Cai, Yujun Lin, Xiuyu Li, Chenfeng Xu, Kelly Peng, et al. Sparse videogen2: Accelerate video generation with sparse attention via semantic-aware permutation. *arXiv preprint arXiv:2505.18875*, 2025.
- [10] Peiqi Yin, Jiangyun Zhu, Han Gao, Chenguang Zheng, Yongxiang Huang, Taichang Zhou, Ruirui Yang, Weizhi Liu, Weiqing Chen, Canlin Guo, et al. vllm-omni: Fully disaggregated serving for any-to-any multi-modal models. *arXiv preprint arXiv:2602.02204*, 2026.
- [11] Jintao Zhang, Jia Wei, Haofeng Huang, Pengle Zhang, Jun Zhu, and Jianfei Chen. Sageattention: Accurate 8-bit attention for plug-and-play inference acceleration, 2025.
- [12] Peiyuan Zhang, Yongqi Chen, Runlong Su, Hangliang Ding, Ion Stoica, Zhengzhong Liu, and Hao Zhang. Fast video generation with sliding tile attention. *arXiv preprint arXiv:2502.04507*, 2025.
- [13] Min Zhao, Guande He, Yixiao Chen, Hongzhou Zhu, Chongxuan Li, and Jun Zhu. Reflex: A free lunch for length extrapolation in video diffusion transformers. *arXiv preprint arXiv:2502.15894*, 2025.
- [14] Min Zhao, Hongzhou Zhu, Yingze Wang, Bokai Yan, Jintao Zhang, Guande He, Ling Yang, Chongxuan Li, and Jun Zhu. Ultravico: Breaking extrapolation limits in video diffusion transformers. *arXiv preprint arXiv:2511.20123*, 2025.